Textural and conoscopic studies of chiral liquid crystals possessing cholestric - smectic A or cholesteric-TGB A - smectic A phase transitions

Yu.A.Nastishin[1,2], M.Kleman[2], O.B.Dovgyi[1]

[1] Institute of Physical Optics, 23 Dragomanov Str., L'viv 79005, Ukraine
[2] Laboratoire de Mineralogie-Cristallographie, Boite 115, 4 place Jussieu, 75252 Paris Cedex 05, France

Received 09.11.2001

Abstract

There exists a well documented analogy between the phase transitions cholesteric – smectic *A* and normal metal − superconductor in the magnetic field. According to this analogy any chiral liquid crystal (CLC) material exhibiting the smectic *A* phase can be subscribed either to I or II smectogenic type as a liquid crystal analogue of the superconductor of I or II type, respectively. In this paper we describe our results aimed to develop a simple identification procedure to establish the smectogenic type of CLC material using only a polarization microscope.

Key words: liquid crystals, conoscopic patterns, phase transitions

PACS: 61.30.Jf, 61.72, 64.70.Md

1. Introduction

Optical microscopy is one of the most powerful tools in characterizing liquid crystal (LC) materials. Most of the discoveries in the liquid crystal physics were inspired by textural observations. Traditionally a study of textural transformations is an unique technique for the express identification of the LC phases in new materials. In many cases one can deduce the internal structure of LC phase analyzing textures of defects. The orientational order parameter of LC as well as secondary order parameters are very sensitive to the external actions. As a result confined LC samples often contain the distortions and topological defects of the director field. Each LC phase exhibits its own set of characteristic defects. The characteristic defects are those which exist only in a given phase, i.e. these defects appear and disappear at phase transitions. The topological defects and accompanied distortions produce specific textures when they are observed between the crossed polarizers under the polarization microscope (PM). Therefore, following defect transformations under PM one can determine the temperature of the phase transition and identify the LC phase. Most of LC phases have their distinctive textures. However, often the characteristic defects are masked by the defects common for LC phases which are neighbors on the phase diagram or which have the same primary order parameter and differ only by their secondary order parameters. The analysis of such textures is complicated and often ambiguous. This difficulty might explain the absence of an effective identification procedure for the so-called Twist Grain Boundary (TGB) Phases. The TGB phases are LCs in which the director field is macroscopically twisted as in a cholesteric phase (N*), while locally the molecules have positional smectic order. In contrast to the N* phase, where molecules continuously rotate around the helical axis, in the TGB phases the three-dimensional smectic

slabs of sizes, much larger than the molecular length, rotate discretely producing a space lattice of screw dislocations [7]. The TGB phase with local smectic A (SmA) is called TGBA phase. The TGBA might appear as an intermediate phase between N* and SmA phases. Returning to the identification problem we stress that the textural identification of the phase transition N*-TGBA is not an easy task. Since the defects are induced by the surface anchoring conditions, as a matter of fact the identification procedure can be successful only in special beneficial geometries which produce the isolated characteristic defects. This paper reports on optical observations of nontrivial pretransitional phenomena, evidenced by defect transformations at the cholesteric (N*) ↔ smectic A (SmA) transition in cholesteryl nonanoate (CN), in several geometries: suspended droplets with tangential anchoring conditions, free standing films, and films with one free surface. The defects observed in CN are akin in all details to those of tolane compound T10 (see [1] for its chemical nature), a material which is known to have the TGBA phase (also termed helical SmA). TGBA's have been under study for 10 years already, but yet little investigated for the nature of their defects. The purpose of this paper is precisely, on the basis of a comparison between the defect textures in CN, T10, CT (cholesteryl tetradecanoate), and chiralized 8CB (4-cyano-4'-octylbiphenyl), a)- to conclude the similar nature of phase transitions in CN and T10, different from those in the two other materials, CT and chiralized 8CB, b)- to characterize novel defects, proper to the TGBA phase. They certainly bear a resemblance to N* defects, but carry definite differences. A theoretical approach to TGBA defects will be given in a forthcoming paper [2].

CT, and 8CB doped by CT, exhibit the first order N* ↔ SmA transition. On the other hand, CN is considered as a standard example of a *weakly* first order N* ↔ SmA transition, and some effort has been made at the time to investigate pretransitional effects in this compound (X-ray scattering measurements of the smectic order parameter [3], pitch and elastic constant divergences [4, 5], etc.). The smectic order parameter is a complex number, and both McMillan [3b] and de Gennes [6] noticed the analogy with the normal metal ↔ superconductor transition.

The TGBA phase is in fact an analogue of the Abrikosov phase. Let us recall that the structure of the TGBA phase consists of SmA slabs of finite constant size, rotated one with respect to another by a finite constant angle about an helical axis (χ axis), parallel to the smectic layers. The boundary between adjacent slabs is a twist grain boundary (TGB) made of parallel equidistant screw dislocations of the SmA phase, which we can term *vortex* lines, for the reason of the analogy with vortices in superconductors. This model is due to Renn and Lubensky [7], prior to any experiment. It has been successfully documented in several materials, on the basis of X-ray scattering, light selective reflection and freeze-fracture observations [8]. In addition, a new phase, NL*, described as a TGBA phase with melted (liquid-like) vortex lines has been proposed [9]. The phase sequence N* ↔ NL* ↔ TGBA has been observed in T10, see [8d]. TGBA textures have been little investigated as yet, except [8e] in the Grandjean wedge geometry.

2. Experiment and discussion

2.1. Materials. Cholesteryl nonanoate (CN, also known as cholesteryl pelargonate), cholesteryl tetradecanoate (CT, also known as cholesteryl myristate) and 8CB (4'-octyl-4-biphenylcarbonitrile) were obtained by Aldrich and used without additional purification. The CN compound transition temperatures on cooling are: I (89.7 °C) N* (T_C = 71.0 °C) SmA (40 °C) Solid Crystal. The N*↔ SmA transition of CT is observed at 77.6 °C. The 8CB+CT 1% wt mixture has a cholesteric pitch of few μm at the N*-SmA transition, comparable to the

corresponding value in CN. T10 [(R)–3–fluoro-4–(1–methylheptyloxy)–4'–(4"–decyloxy–2",3"–difluorobenzoyloxy)tolane] was characterized in [8d,e]. The temperature was controlled and measured by the Mettler hot stage (0.1 °C accuracy).

2.2.Freely suspended droplets.

Experiment. The *freely suspended droplets* were prepared in 400 μm thick flat capillaries (Vitrodynamics) by mixing powder with glycerol. Far away from the N* ↔ SmA transition the N* droplets of CN, CT and T10 have the structure of Robinson spherulites [10], see Fig. 1a, with a disclination radius of strength k=2 (4π rotation of the cholesteric local trihedron of directors about the disclination [11]) extending from the boundary of the droplet to a terminal point in the center of the droplet (N* defects of strength k = 2 can escape to a zero defect [12]). The analogy of this defect structure with a Dirac monopole attached to a string has been emphasized [13]. The optical contrast of the defect line is poor at high temperature, (Fig. 1a), and increases on cooling, as the pitch increases, (Fig. 1e). The droplets display a Maltese cross between crossed polarizers – four black brushes crossing at the center of the droplet (Fig. 1a, CN, ΔT > 1°C). This texture is characteristic of spherical cholesteric layers when the anchoring conditions are planar [14]. The droplet texture does not depend on its size, except for very large droplets flattened between two surfaces, which are outside the present investigation. The CT droplet

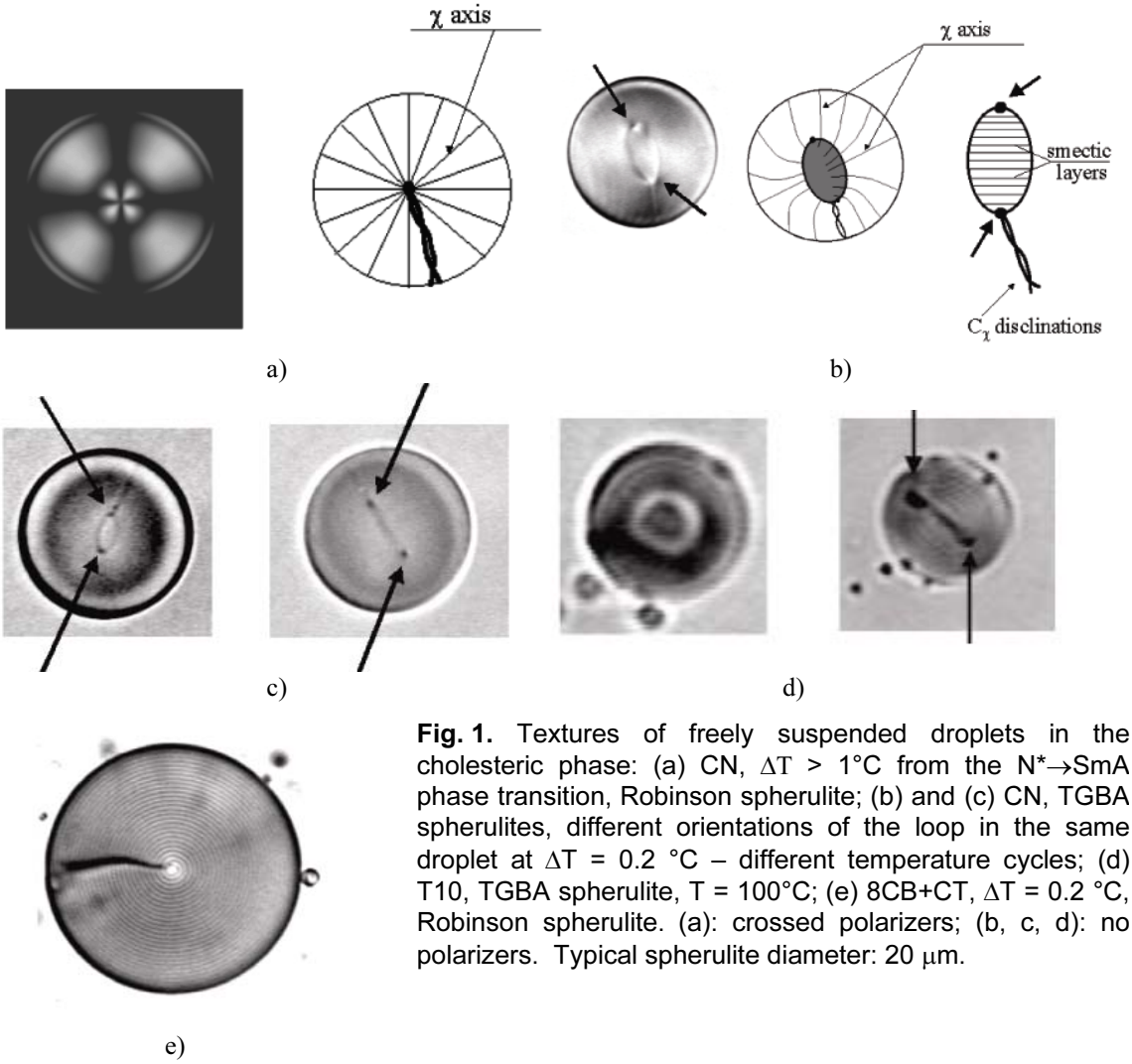

Fig. 1. Textures of freely suspended droplets in the cholesteric phase: (a) CN, ΔT > 1°C from the N*→SmA phase transition, Robinson spherulite; (b) and (c) CN, TGBA spherulites, different orientations of the loop in the same droplet at ΔT = 0.2 °C – different temperature cycles; (d) T10, TGBA spherulite, T = 100°C; (e) 8CB+CT, ΔT = 0.2 °C, Robinson spherulite. (a): crossed polarizers; (b, c, d): no polarizers. Typical spherulite diameter: 20 μm.

texture does not change upon cooling down to the transition to SmA. In CN, at $T_1 = T_c+1°C$, and in T10, at T= 105.8°C (where the NL* phase is expected), the central terminal point of the defect splits into a planar, slightly anisometric loop, (Fig. 1b,c), attached to the disclination radius. The beginning of this transformation manifests itself as a splitting of the Maltese cross (Fig.1a) into two sets of two mutually orthogonal brushes. Incidentally, one may wonder whether the Dirac monopole also possesses a 'point' state and a 'loop' state. The region inside the loop has a uniform color, due to a selective reflection from the helical structure, when the plane of the loop is perpendicular to the microscope axis. This indicates that the director orientation is uniform in this plane. The diameter of the loop scales approximately as the size of the droplet and can be much larger than the pitch. The loop size is stable as long as the temperature is constant, and increases as the temperature is lowered. There are two diametrically located point defects on the loop (shown by arrows in Fig. 1b, c, d). They are poorly visible when the loop plane is perpendicular to the microscope axis, and better contrasted when it is parallel to the microscope axis. They scatter the light, being visible without polarizer and analyzer. Their position does not move along the loop under defocussing. Such features imply that these points are singular point defects. We believe that these two points mark the termination of the parallel smectic layers in the plane of the loop, as it is shown in (Fig. 1b). It is observed that near the phase transition that the disclination radius is split into two defect lines wound into a double helix and connected by the loop in the central region of the droplet. The diameter of the loop increases by mechanical rotation of the structure of the droplet around the line defect, whose effect is to unwind the double helix. As a result the plane of the loop has a random orientation with respect to the plane of the capillary limiting surfaces (Fig.1b,c,d). Although we observed that on cooling in the T10 droplets the diameter of the loop increases much quicker as the temperature passes through the value T=103.1°C, where according to [8c, d] the NL* $\rightarrow$ TGBA phase transition is expected, we were not able to identify this temperature point unambiguously. The texture transformations are reversible in the temperature and can be followed on heating. We conclude that (Fig.1b,c,d) shows a texture characteristic of the TGBA phase. This conclusion is supported by the fact that this texture does not appear for CT and CT+8CB droplets, Fig. 1e, and was never reported for N*. In (Fig. 1e) we present the evidence that in the absence of the TGB phase between the cholesteric and the smectic A phases (which is the case of chiralized 8CB) the size of the central region is of the order of the pitch and no loop is observed.

Let us remark that a λ (k=1/2) disclination loop can be observed for cholesteric droplets flattened between two substrates (see [14]). But this type of loop has no relationship with our observations. In flattened cholesteric droplets the plane of the loop is the result of a stress and is parallel to the limiting substrates. It is not the case for the CN and T10 droplets described above. We checked that the described textures do not result from the contact with limiting substrates. Moreover in our case the plane of the loop rotates around the χ disclination lines when the temperature is changed. Fig. 1 shows different orientations of the loop obtained in different temperature cycles.

The N* k = 2 line is transformed in TGBA as follows. In the Frank and Pryce model of the N* Robinson spherulite, the disclination is a k=2 wedge; Fig. 18 of [14] shows the λ director projection in a section perpendicular to the disclination (not much different from the true director in a section far enough from the center of the spherulite). The non-singular N* disclination radius is obtained as a small distortion of this geometry. Since the helical axis χ is vertical (in this picture), the smectic

layers project along lines perpendicular to the λ director, i.e. along lines displaying the same geometry as the λ director, but rotated by $\pi/2$. By slightly distorting the configuration, as in Fig. 18b in [14], the smectic layers can be made parallel, at the expense of a larger distance between the two (helically shaped) $k = 1$ branches of the $k = 2$ line, however not much larger than the pitch. We believe that this is the principal (and essential) effect of the phase transition on the disclination radius.

On the other hand, the singular point of the χ field, at the center of the spherulite, suffers a considerable change; it opens up into two $|k|=1/2$ lines, both joining the two terminations of the two branches of the $k = 2$ disclination radius (Fig.2). Because of the group relations between the elements of Q, the two $|k| = 1/2$ lines must belong to the same conjugacy class of Q. Let $C\lambda$ (resp. $C\tau$, $C\chi$) be the class of the two $|k| = 1/2$ lines with a non-singular

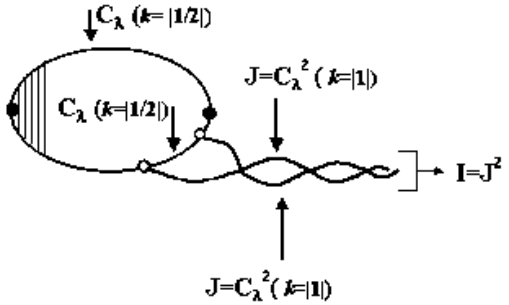

Fig.2. Schematized representation of the topological relations between the disclination loop and the disclination radius.The quaternion group is a non-abelian group with 8 elements (**I**, the identity element, corresponding to any defect whose rotation angle is multiple of 4π, I***k***I=2; **J,** angle 2π, I***k***I=1; σ_λ and σ_λ^{-1}, angle π, I***k***I=1/2; etc…, with relations of the type $\sigma_\lambda\sigma_\tau = \sigma_\chi$, $\sigma_\tau\sigma_\lambda = \sigma_\chi^{-1}$, etc…?These elements form 4 classes of conjugacy; **I** and **J**, which are classes by themselves; $\mathbf{C}_\lambda$ (σ_λ^{-1} and σ_λ); $\mathbf{C}_\tau$ (σ_τ^{-1} and σ_τ); $\mathbf{C}_\chi$ (σ_χ^{-1} and σ_χ). The product of two elements belonging one to $\mathbf{C}_\lambda$, the other to $\mathbf{C}_\tau$, say, belongs to $\mathbf{C}_\chi$: $\mathbf{C}_\lambda\mathbf{C}_\tau = \mathbf{C}_\chi$. Similarly $\mathbf{C}_\chi\mathbf{C}_\tau = \mathbf{C}_\lambda$, $\mathbf{C}_\lambda\mathbf{C}_\chi = \mathbf{C}_\tau$, $\mathbf{C}_\lambda^2 = \mathbf{C}_\chi^2 = \mathbf{C}_\tau^2 = \mathbf{J}$ or **I**.

λ (resp. τ, χ) director in the core; τ is not materialized, in N* as well as in TGBA. Therefore both defect classes $C\lambda$ (resp. $C\chi$) carry only one type of singularity, viz. a χ (resp. a λ) singularity. The class $C\tau$ carries χ and λ singularities. We, therefore, advance the idea that the $k = 1$ terminations are linked by a short $C\lambda$ line segment, (size ≅ p), and a long $C\lambda$ loop segment (see Fig.2). The global geometry opposes the presence of a $C\chi$. The λ director is uniformly oriented inside the loop (perpendicular to the smectic layers, Fig.1b) which is slightly elongated in the direction of this director, in order to facilitate a λ non-singular geometry in the core, i.e. favoring a wedge $C\lambda$ line *vs* a twist $C\lambda$ line. The extremities of the loop are therefore locations of stronger singularities, and are preferred locations for the short segment. These singularities are often observed.

2.3. Free Standing films.

Fig.3. shows defects observed in *free standing films*, prepared inside 42 μm × 42 μm squared holes of standard electron microscopy copper grids, a technique recently used for nematic thin films [15]. The thickness of the films is estimated ≅ 5μm. Starting from the SmA phase of CN and increasing the temperature, one grows a regular texture with χ axis in the plane of the film, almost everywhere perpendicular to the nearest edge of the limiting square, Fig.3a. Such alignment of the χ axis produces four diagonal tilt grain boundaries of the slabs and a k=1 line singularity of the χ director in the center of the square. This singularity splits into two singular lines k=1/2, from which two spirals extend through the sample. The same texture was obtained for T10 below T=103°C, where a TGBA phase is expected, Fig.3b. Additional new defects appear upon heating, at T_1, the TGBA→NL* phase transition. This transformation will be discussed elsewhere. In both cases,

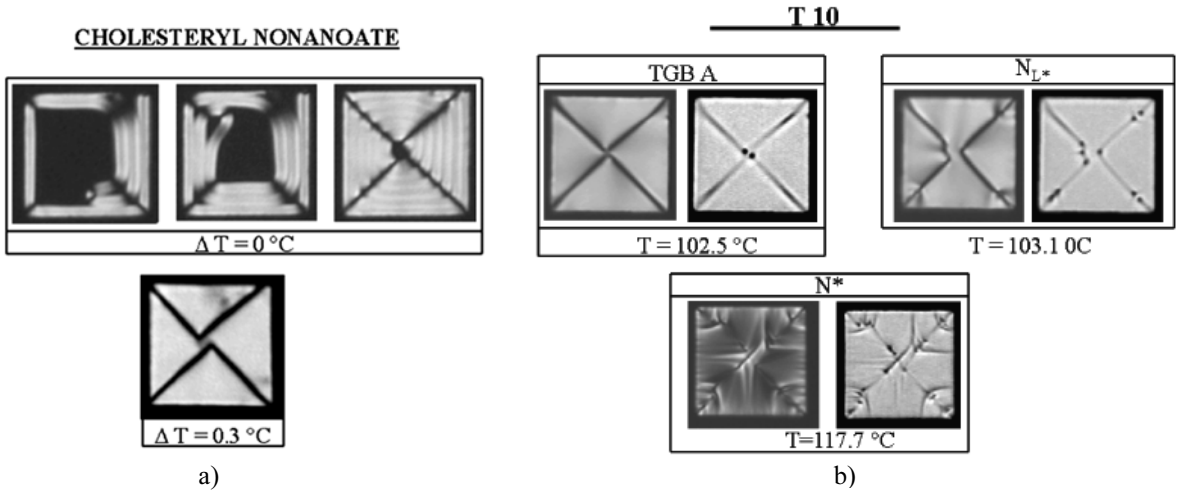

a) b)

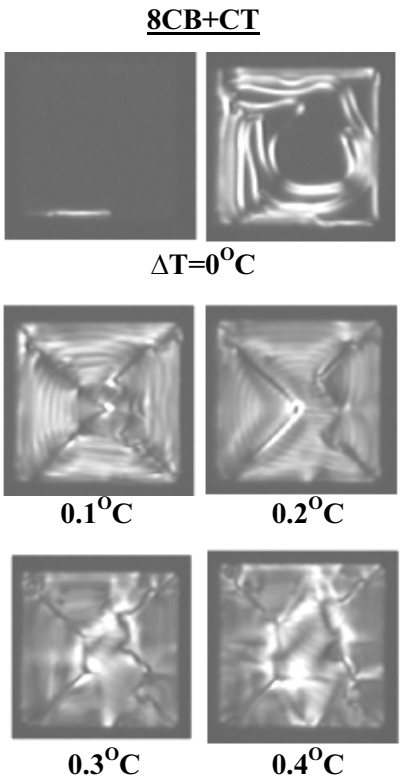

c)

Fig. 3. Free standing films on a square grid, edge length 42 μm.

viz. CN and T10 films, the film of uniform color, observed between the crossed polars, shows that the direction of the film thickness averaged optical axis i.e., the χ axis, is strictly in the plane of the film and strongly oriented.

It is known that at a scale larger than p, the layer thickness is nearly constant in the N* phase: the lines of force of the χ director are nearly straight and one observes nearly perfect *focal conic domains* (FCD). This constraint should be even stronger in NL* and TGBA. However, FCDs now can be disfavored because the conjugated conics would carry strong singularities of χ. *Developable domains* [16] offer another possibility to keep the layers thickness constant about a wedge disclination as the $k = 1$ line singularity of the χ director in the center of the square; this geometry, akin to what has been observed in columnar phases, is favored, at least in TGBA, the slabs arranging into logarithmic spirals where the distance between TGBs is conserved [2]. This is in contrast with the films of 8CB+CT, where the texture is much more defective, and the color of the film between crossed polarizers changes from point to point, confirming that the 8CB+CT films are in the N* phase, Fig. 3c.

A further evidence - that the local order of CN below T_1 and the local order of chiralized 8CB indeed differ - follows from the flickering of the director observed for chiralized 8CB but not for CN and T10: the thermal fluctuations of the nematic director produce a scintillating contrast of the texture between the crossed polarizers for chiralized 8CB; the CN and T10 textures do not have such a feature.

2.4. Textures in flat cells.

Chiral nematics confined between two transparent parallel plates (with or without special surface treatment) display several typical

textures, which allow to identify this phase by the polarization microscopy.

Planar anchoring. At planar anchoring conditions the optical axis is along the microscope axis. Without defects this texture is optically active, selectively reflects light. The optical properties of the NL*, TGBA phases are the same as the properties of the cholesterics. Therefore, the uniform planar anchoring conditions do not allow to distinguish between cholesteric and N_L*, TGBA phases. Typical defects of the planar cholesteric texture are oily streaks. The structure of the oily streaks is complicated and can be accompanied with many defects of different types. Although one can see that at the phase transitions N*-TGBA the oily streak texture changes, but it is not easy to identify these structural transformations. The observations of the isolated defects are usually more conclusive. Other defects with low textural contrast are also not of practical use. Therefore, the analysis of the planar texture is not convenient for the identification of the phase transformations between N*, NL* and TGBA phases.

Homeotropic and hybrid anchoring. Homeotropic and hybrid anchoring conditions for the N* phase produce three typical textures depending on the pitch/thickness (P/d) ratio.

P<<d. When the pitch is much smaller than the sample thickness, the cholesteric can be considered as a lamellar system of equidistant layers. The typical defect of the lamellar system is a Focal Conic Domain (FCD). At homeotropic and hybrid anchoring the small pitch cholesterics form the FCD texture. Between the crossed polarizers this texture often looks as a set of Maltese crosses. The FCD texture can be easily obtained by placing a cholesteric on glycerol (hybrid conditions) or on a substrate with homeotropic alignment. A cholesteric between two solid substrates, producing homeotropic or hybrid alignment, has qualitatively the same textures, but the films with degenerated azimutal anchoring are more convenient for the observations. When the cholesteric transits to the NL* phase, the cholesteric layers become composed by smectic blocks parallel to the helical axis and rotating around it. Because of the local smectic order (contrary to the cholesterics, which are locally nematic) the «cholesteric (NL*)» layers become more rigid. After transition to the NL* or TGBA phase the defect lines of FCD (ellipse and hyperbola) become the regions of strong mismatches for smectic blocks, and the system escapes from the FCD geometry. This transformation is well observed in the CN films on glycerol, as well as on a solid substrate near the transition to the TGBA phase, as a splitting of the Maltese crosses into two pairs of orthogonal brushes.

Another possibility for packing quasi-equidistant layers is a cylinder. Cholesteric layers packed in a cylinder are called fingers or strips. Even in the cholesteric phase the structure of the fingers is complicated. Generally, the cholesteric finger is not circular and is based on a closed curve of the shape dependent on many material and geometrical parameters. In the cholesteric phase the fingers are of random in-plane curvature creating the so-called «fingerprint texture». The textural transformation at the phase transition N* – TGBA (NL*), described in the previous paragraph is the transformation from the FCD geometry to the finger geometry of the «cholesteric» layers. In the NL* and TGBA phase the fingers are much more rigid than in the cholesteric phase, and instead of forming a random «fingerprint texture» the TGB(NL*) fingers form developable domains (DD). In this paper we discuss only the general topological properties of the NL* and TGBA finger packing without going into details of the internal finger structure. This study is in progress. The observation of the DDs in the TGBA phase first was reported in [19]. The DDs are typical defects of the columnar phases. In a columnar phase the columnar organisation of the disc-like molecules

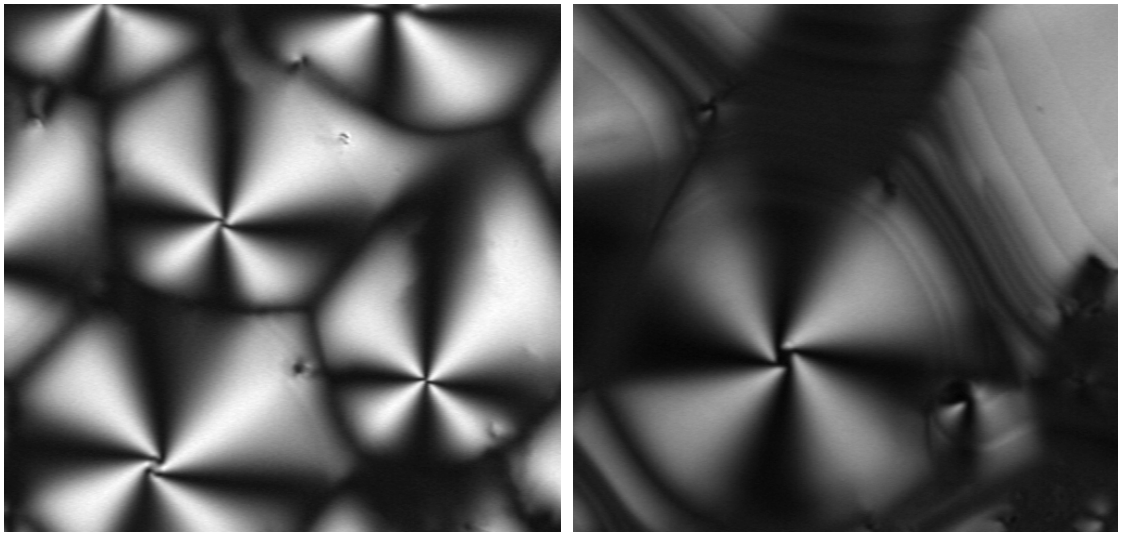

a) b)

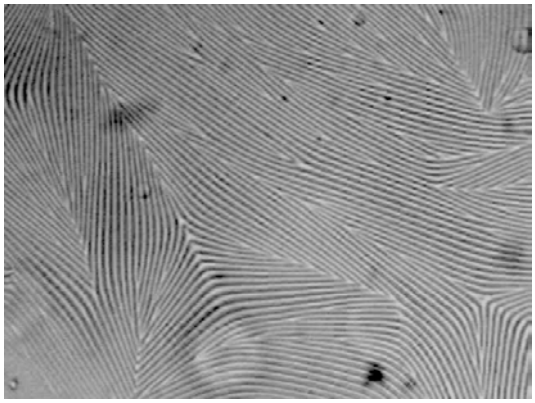

c)

Fig. 4: a)Texture of developable domains (DD) type, b) the core of DD is circular, c) Tilting Grain Boundaries (TiGB) formed by the TGB fingers

is the intrinsic property of the phase. The strongly curved columns in the columnar phase relax to the DD geometry. In the NL* and TGBA phase a DD is a secondary structure formed by the fingers. This conclusion follows also from the fact that the DDs appear for two different anchoring conditions: homeotropic and hybrid. If the DDs were the result of the intrinsic columnar structure of the TGBA phase, as it was proposed in [19], it is not very plausible that such a very different arrangement of the columns, which should take place at hybrid and homeotropic anchoring, can produce the same texture, namely the DD texture. We believe that it is a finger that plays a role of a column in the NL* and TGBA phase. However, since the internal structure of the fingers depends on the confinement conditions, in contrast to the columnar phase in the NL* and TGBA phases the DDs are often strongly distorted and accompanied by other defects. By temperature cycling of the sample from the TGBA phase to the Sm A phase and back we were able to eliminate the majority of the distortions of the DD's. The Fig. 4a,b show the DDs obtained in such a way in the CN films on glycerol. The circular core of the DDs is clearly visible (Fig.4b). The cores of the DDs are filled by homeotropic Sm A. This statement becomes evident by observing the process of the formation and further temperature transformations of the DDs. Since the width of the finger is defined by the pitch, one can hope to visualize the spiral packing of the fingers, starting from almost ideal DDs shown in Fig.4a,b, and cooling down to the temperature when the fingers can be recognised by the microscope. However, it turns out that the intrinsic transformations inside the fingers, which take place on cooling, induce transformations of the DDs. The transformations of the DDs on cooling are very mobile and are accom-

panied with the in-plane flow of the structure in the films on glycerol. It appears to be quite difficult to follow the temperature transformations of a given DD in films. For CN on solid substrate covered by rubbed polyimide the flow of the structure is much smaller and we were able to observe spiral packing of the fingers in DDs «frozen» by strong anchoring. However because of the rigidity of the fingers they are interrupted in many places. This fact also shows that the DD is stable only at special conditions and is a secondary organisation of the fingers.

The DD plays the same role for the NL* and TGBA phase as a FCD does for short pitch cholesteric. The developable domains can be observed in the NL* and TGBA phase at the same confinement conditions which favour the FCD texture in cholesterics, namely: weak homeotropic anchoring, d>>P. Typically for the samples of several micron thickness the pitch has to be smaller than 1μm.

P ≈ d. When *P* becomes comparable to *d,* then DDs become unstable against splitting into two ½-defects. The transformation of DD's into ½-defects is also typical for columnar phase. On the further increasing of the pitch the fingers become more and more straight forming TiGBs (Fig. 4c). Typical cholesteric fingerprint texture taking place at weak homeotropic anchoring conditions, when the pitch is comparable to the sample thickness, is quite distinguishable from DD's and TiGB textures of the TGBA phase. This difference can be used for the identification of the TGB (NL*) phase.

P>d. When P/d>1 the helical structure becomes unwound, extinct between crossed polarizers. The unwound structure of the N* phase is actually homeotropic nematic, and the unwound structure of and TGBA (NL*) phase is the homeotropic smectic A. A clear difference between unwound textures of N* and TGB phases can be observed in thick samples. The director flickering producing scintillated contrast is observed in the N* phase, and no such feature exists for the TGBA phase.

The textural transformations at the hybrid and homeotropic anchoring confinement that help to identify the transition N* - (NL*)TGB A are summarized in the table.

As an indication of pretransitional effects in the SmA phase, let us stress that FCDs do not appear spontaneously on cooling; instead we observe screw dislocations of giant Burgers vectors (Fig.5), as in [20], and a texture shown in Fig.6. This seems to indicate some continued penetration of twist. SmA phases like CT and 8CB+CT, even in a very distorted homeotropic sample, do not display such an anomaly.

The conoscopic pattern of homeotropic SmA for CN also differs from the pattern that is expected to be observed for the uniaxial crystal (Fig.7). The homeotropic orientation was obtained between two glass substrates by shifting the upper substrate. The polarization microscopy does not display presence of visible defects and distortions. We checked that the SmA cells of nonchiral material 8CB oriented in the same way, did not display such a pattern even for very distorted samples. Fig. 7 demonstrates that the SmA phase of a chiral material differs from the Sm A phase in a non-chiral material.

Table 1.

	N*	NL*	TGB A
d>>P	Confocal texture	Developable domains	Distorted developable domains
d≈P	Cholesteric fingerprint	Half-developable domains	TiGB of straight fingers
d<P	Homeotropic nematic	Probably homeotropic smectic A	Homeotropic smectic A

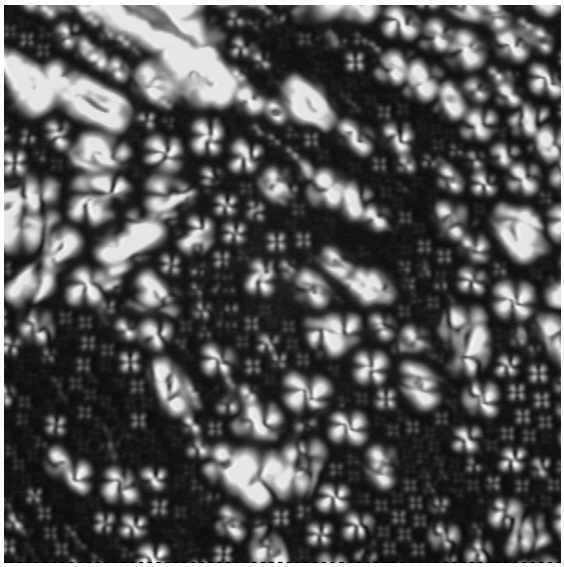

Fig. 6. Texture of SmA film with one free surface for CN.

2.4. Some comments.

The remarkable similarity of the textures of defects in the CN phase and in typical 'type II' materials like T10 at the N* → SmA transition calls for a reappraisal of the well-known pretransitional properties of CN, and a closer look at T10 from this point of view. McMillan [3a] advanced a theory where the interaction constants of CN place it at the boundary between a 1st and a 2nd order transition, in

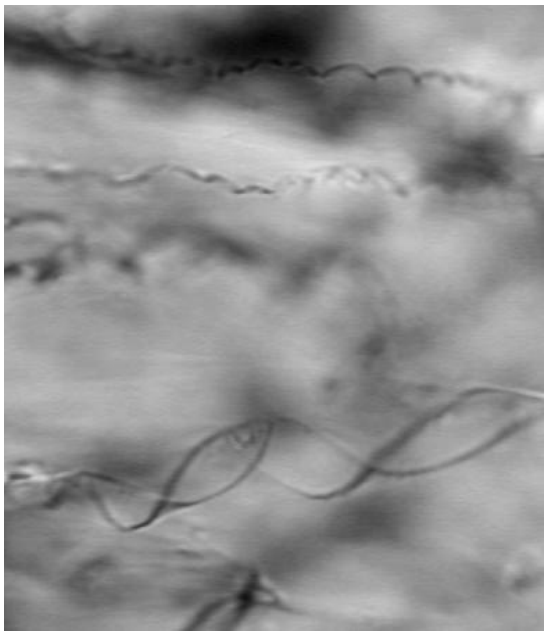

Fig.5. Screw disclinations of giant Burger's verctor in the SmA phase of CN.

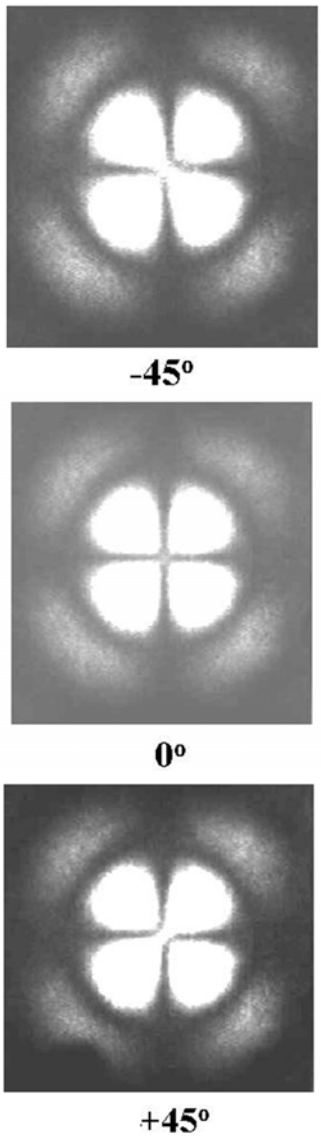

Fig. 7. Conoscopic pattern for the homeotropic SmA of CN near the phase transition to the TGBA phase. The homeotropic orientation was obtained by shifting one of the substrates. The angle between the shifting direction and the polarizer is indicated under each photo.

contrast to CT (definitely 1st order). Two remarks are of interest: a)- the Ginzburg parameter κ_2 for CN, calculated in [17] on the basis of very small latent heat for CN, and of other material parameters [3b, 5], is practically equal to $1/\sqrt{2}$. This supports the possibility of the existence of the Abrikosov phase in the vicinity of the phase transition; b)-the difference between N* ↔ SmA transition types in CN and CT probably, originates in the fact that the CT

molecule is longer (as shown in [17], the width of the N phase decreases with molecular length in a nonchiral homologous series).

The examination of defects does not yet give a clear-cut answer to the question of the existence of a melted Abrikosov phase (except some indication in free standing films). On the other hand, DSC experiments show that the peak corresponding to the transition to the SmA phase in the CN is anomalously broad, and its amplitude is very dependent on the scanning rate. This is reminiscent of the situation in T10 [8e]. For CN, at a cooling rate of 0.1 °C/min the amplitude of the peak is only slightly larger than the amplitude of the noise signal. The width of the peak and its intensity scanning rate dependence imply that the peak might result from several phase transformations including N* $\leftrightarrow$ NL* and the weakly first order NL* $\leftrightarrow$ TGBA transitions.

Acknowledgements. We acknowledge the assistance in experiments and discussion with Sophie Asnacios and Claire Meyer, L.Pelykh, as well as discussions with Brigitte Pansu and Oleg Lavrentovich.

References

1. A. Bouchta *et al.*, Liquid Cryst., **12**, 57S (1992).
2. M. Kleman, Yu. A. Nastishin and J. Malthête, in preparation.
3. W. L. McMillan, a)- Phys. Rev. A **4**, 1238 (1971), b)- Phys. Rev. A **6**, 936 (1972).
4. P. Kassubek and G. Meier, Mol. Cryst. Liquid Cryst. **8**, 305 (1969).
5. R. S. Pindak *et al.*, a)- Solid State Commun. **15**, 429 (1974); b)- Phys. Rev. Lett. **32,** 43 (1974).
6. P. G. de Gennes, Solid State Commun., 10 (1972) 753.
7. S. R. Renn and T. C. Lubensky, Phys.Rev. A **38**, 2132 (1988).
8. a)- J. W. Goodby *et al.*, Nature **337**, 449 (1989); b)- O. D. Lavrentovich *et al.*, Europhys. Lett. **13**, 313 (1990); c)- K. J. Ihn *et al.*, Science, **258**, 275 (1992); d)- L. Navailles *et al.*, J.Phys. II France **6**, 1243 (1996); e)- N. Isaert *et al.*, J.Phys. II France **4**, 1501 (1994).
9. R. D. Kamien and T. C. Lubensky, J.Phys. II France **3**, 2131 (1993).
10. M. H. L. Pryce *et al.*, *in*:Robinson C *et al*., Disc. Faraday Soc. **25**, 29 (1956).
11. a)- J. Friedel and M. Kléman , J. de Phys., **30**, C4:43 (1969); b)- M. Kléman, *Points, Lines and Walls*, Wiley, 1983.
12. G. E. Volovik and V. P. Mineyev, Sov. Phys. JETP Lett. **45**, 1186 (1977).
13. see e. g. M. V. Kurik and O. D. Lavrentovich, Sov.Phys. JETP **58**, 299 (1983).
14. Y. Bouligand and F. Livolant, J. de Phys., **45**, 1899 (1994).
15. V. G. Nazarenko and A. Nych, Phys. Rev E **60**, R3495 (1999).
16. M. Kleman, J. de Phys., **41**, 237 (1980).
17. P. B. Vigman and V.M. Filev, Sov. Phys. JETP **42**, 747 (1976).
18. W. L. McMillan, Phys. Rev. A**7**, 1419 (1973).
19. C. E. Williams, Phil. Mag., **32**, 313 (1975).
20. A.C.Ribeiro, A. Dreyer, L. Oswald, J.F.Nicoud, A.Soldera, D. Guillon and Y.Galerne, *J. Phys. II France* 4 (1994) 407-412